Electronic Supplementary Material (ESI) for ChemComm.

Supporting Information

A disordered tether to iLID improves photoswitchable protein patterning on model membranes

Daniele Di Iorio,* Johanna Bergmann, Sayuri L. Higashi, Arne Hoffmann, and Seraphine V. Wegner*

Materials

All lipids were purchased from Avanti Polar Lipids as powder or already dissolved in chloroform. The membrane dye 1,1′-dioctadecyl-3,3,3′,3′-Tetramethylindodicarbocyanine (DiD, catalog number D7757-10 mg) was purchased from Thermo-Fisher Scientific. All others chemicals were purchased from Sigma Aldrich. All microscopy experiments for GUV were performed in μ-slide 18-well glass bottom chambers from ibidi (Cat. # 81817).

Plasmids

The plasmids pQE-80L iLID (C530M) and pQE-80L MBP-SspB Nano were gifts from Brian Kuhlman (Addgene # 60408 and 60409, respectively).[1] A pET-21a(+) plasmid containing the gene for dis-iLID (pET21_dis-iLID) between the cloning sites NdeI and HindIII was bought from GenScript. The mOrange was inserted into the pQE-80L MBP-SspB Nano plasmid after the BamH1 cutting site to yield His6-MBP-TEV-mOrange-Nano, as previously reported.[2]

pQE-80L iLID was digested with EcoRI and BamHI, ligated with synthesized dsDNA coding for an AviTag and an hexahistidine (His6-) tag presenting EcoRI and BamHI overhangs and transformed in *E. coli* DH5α to yield pQE-80L iLID-AviTag. (5′-AATTCATTAAAGAGGAGAAATTAACTATGGGTGGTTCCGGCCTGAACGATATC TTCGAAGCGCAGAAGATTGAATGGCACGAAGGTGGTTCCCATCACCATCACC ATCACG-3′ and 5′-GATCCGTGATGGTGATGGTGATGGGAACCACCTTCGTGCCATTCAATCTTCTG CGCTTCGAAGATATCGTTCAGGCCGGAACCACCCATAGTTAATTTCTCCTCTT TAATG-3′)

The synthesized dsDNA for AviTag and a His6-tag presenting NdeI and NcoI overhangs

(5′-
TATGGGTGGTTCCGGCCTGAACGATATCTTCGAAGCGCAGAAGATTGAATGG
CACGAAGGTGGTTCCCATCACCATCACCATCACGGTTC-3′ and 5′-
CATGGAACCGTGATGGTGATGGTGATGGGAACCACCTTCGTGCCATTCAATCT
TCTGCGCTTCGAAGATATCGTTCAGGCCGGAACCACCCA-3′) was ligated into pET21_dis-iLID digested with NdeI and NcoI and transformed in *E. coli* DH5α to yield pET21_dis-iLID-AviTag.
All constructed plasmid DNAs were verified by DNA sequencing.

Methods

Protein expression and purification:

iLID, disiLID, Nano, mOrange-Nano. All the proteins were recombinantly expressed in *Escherichia coli* and purified through their N-terminal His6-tag following reported procedures.[2] The His6-MBP tag of His6-MBP-TEV-mOrange-Nano were removed using TEV digestion to yield mOrange-Nano as previously reported.

Biotinylated-iLID (b-iLID) and biotinylated-disiLID (b-disiLID). To obtain *in vivo* biotinylated proteins, pQE-80L iLID-AviTag and pET21_dis-iLID-AviTag were transformed into the strain BL21(DE3) pBirAcm (Hölzel diagnostics trading GmbH, Germany, Catalogue No.: Avid CYB T7POL). For protein expression an overnight culture was inoculated (1:100) into LB medium supplemented with 50 µg/mL ampicillin and 10 µg/mL chloramphenicol and bacteria were grown at 225 rpm 37 ˚C. For protein expression was induced at OD_{600} ~ 0.6 by adding 1 mM IPTG and 30 µg/mL d-biotin. After induction for 16 h at 30 ˚C, the cells were pelleted by centrifugation (Avanti J-25, Beckman coulter). For purification, the cells were resuspended in 50 mL Buffer A (50 mM Tris-HCl pH 7.4, 300 mM NaCl) supplemented with 1 mM dithiothreitol, 1 mM phenylmethylsulfonyl fluoride, and 1 mg/mL lysozyme and sonicated (Omni Sonic Ruptor 400, OMNI). Cell debris was pelleted by centrifugation. The supernatant was cleared through a 0.25 µm filter, applied to a gravity flow StrepTactin column (IBA GmbH, Catalogue No.: 2-1201-002), and eluted using 50 mL Buffer A with 5 mM *d*-Desthiobiotin. Finally, the protein was concentrated using Amicon® Ultra-15 centrifugal filter device with a 10 kDa cut-off (Merck, Catalogue No.: UFC901008D). The purified protein was analyzed on an SDS-PAGE gel. To confirm biotinylation, after denaturing the

purified proteins at 95 ˚C for 15 min with reducing 4×SDS loading buffer (50 mM Tris-HCl, pH 6.8, 2% SDS, 10% glycerol, 0.01% bromophenol blue, 1.3% β-mercaptoethanol) 1 mg/mL streptavidin were mixed with into the samples after heating. The protein concentration was determined by UV-Vis spectroscopy.

Fluorescence polarization measurements

Fluorescence polarization measurements were performed with a Spark multimode plate reader (Tecan Life Science) using 96-well black bottom plates. The excitation and emission wavelengths were set to 540 nm and 590 nm, respectively, with a bandwidth of 20 nm. First, binding affinity of TAMRA-labeled SsrA peptide (Sequence: AANDENY-TAMRA) towards Nano was determined by titrating of increasing concentration of Nano into 200 nM SsrA peptide in filtered (Filtropur S 0.2 μm) buffer (50 mM Tris pH 7.4, 100 mM NaCl). For the competitive fluorescence polarization assay, 200 nM SsrA-TAMRA peptide and 200 nM of Nano were titrated with increasing concentration of either iLID or disiLID (0-5 μM). The fluorescence polarization was measured first in the dark and subsequently after 60 s blue-light illumination.

Small unilamellar vesicles (SUVs) preparation

SUVs were prepared by adapting previously reported methods.[3] Lipids were first dissolved in chloroform, and solutions of 1 mg/mL 1,2-Dioleoyl-sn-glycero-3-phosphocholine (DOPC) with 5 mol% 1,2-dioleoyl-sn-glycero-3-phosphoethanolamine-N-(cap biotinyl) sodium salt (DOPE-biotin) and 0.1 mol% DiD (where needed) were prepared in glass vials. Afterwards, chloroform was slowly evaporated with a nitrogen stream while rotating the vials in order to form a thin lipid film. The residual chloroform was removed for at least 1 h under vacuum. The dried film was rehydrated in MilliQ water with a final concentration of 1 mg/mL lipids by vortexing. Finally, the obtained solution was sonicated for 10 min until the opaque solution turned clear, indicating the formation of SUVs with size smaller than 100 nm. The obtained SUV solutions were transferred to an Eppendorf tube and stored in the fridge for maximum 2 weeks.

QCM-D measurements

All QCM-D measurements were performed using a Q-Sense E4 system (Q-Sense) on SiO_2 crystals (Q-sense). Measurements were done at 23 ºC and operated with four parallel flow chambers, using one Ismatec peristaltic pump with a flow rate of 75 µl/min. Blue light illumination was done with a blue light bulb (Decospot LED 80005, Osram) through a window chamber. For every measurement, the seventh overtone was reported for the normalized frequency (Δf_7) and dissipation (ΔD_7). Before each measurement, QCM-D crystals were immersed in a 2 wt% sodium dodecyl sulfate (SDS) solution for 30 min, thoroughly rinsed with Milli-Q water and dried under a nitrogen stream. Subsequently, the sensors were placed in an UV/ozone cleaner (Ossila) for 10 min. The cleaned and activated sensors were placed in the QCM-D chambers and buffer (50 mM Tris pH 7.4, 100 mM NaCl) was flushed over the surfaces until a stable baseline was reached. Subsequently, for the formation of SLBs, SUVs were diluted to a concentration of 0.1 mg/mL in buffer supplemented with 10 mM $CaCl_2$ directly before use. The quality of the SLBs was monitored *in situ* by QCM-D, where high quality SLBs are defined by $\Delta f = 24 \pm 1$ Hz and $\Delta D < 0.5\times10^{-6}$. The SLBs were functionalized consecutively with 10 µg/mL Streptavidin (SAv) and 1 µM b-iLID/b-disiLID in buffer. After each functionalization step, the system was washed with buffer until a plateau was reached. For the titration with Nano, the readily functionalized SLB was consecutively flushed with solutions of increasing protein concentration (blue light condition: 10 nM, 20 nM, 50 nM, 100 nM, 200 nM; dark condition: 100 nM, 200 nM, 500 nM, 1000 nM, 2000 nM).

Confocal microscopy measurements

All images were acquired on a Leica SP8 confocal laser-scanning microscope through a 63× water objective. The mOrange-Nano was excited with a 552 nm laser, and the emission was detected at 570nm - 608nm; the DiD dye was excited with a 638 nm laser, and the emission was detected at 665nm - 724nm. The photoactivation of iLID was achieved with a 488 nm laser. All images were analyzed using Leica Application Suite X (LAS X) and quantified with ImageJ (for the GUVs) or with LAS X (for SLBs).

mOrange-Nano Recruitment to disiLID/iLID functionalized GUVs

GUVs were prepared using the assisted gel GUV formation method.[4] A 5% (w/v) polyvinyl alcohol (PVA) (MW: 145 000 g/ mol) solution with 100 mM sucrose was prepared in Milli-Q water overnight at 80 °C at 400 rpm. Then, 40 µL of PVA solution was spread as a thin layer on top of a 60 x 24 mm glass slide and dried at 50 ºC for 30 min. Afterwards, 5 µL of a lipid solution (10 mg/mL POPC, 10 mol% 1-palmitoyl-2-oleoyl-sn-glycero-3-phospho-(1'-rac-glycerol) (POPG), 2 mol% DOPE-biotin and 1 mol% DiD) in chloroform were spread and dried on the PVA layer at 30 ºC. Subsequently, a chamber was assembled on the functionalized slide using a Teflon spacer (ca. 40 mm × 24 mm × 2 mm) and a second glass slide. The GUVs were formed by adding 1 mL of rehydration buffer (50 mM Tris pH 7.4, 100 mM NaCl) into the chamber for 1 hour at room temperature. The chamber was inverted to harvest the GUVs. An excess of 0.15 µM SAv was added immediately to the freshly harvested GUVs. After 30 min, 1 µM of either b-iLID or b-disiLID was added to the GUVs solution and the solution was incubated for 30 min in the dark.

Afterwards, 5 µL of GUVs decorated with disiLID or iLID were mixed in the dark with 145 µL of 200 nM mOrange-Nano in buffer (50 mM Tris pH 7.4, 100 mM NaCl) in a BSA (3 wt. %) pre-treated µ-slide 18-well glass bottom chamber. The GUVs were located under the confocal microscope using the DiD channel and the recruitment of mOrange-Nano (λex = 557 nm; λem = 576 nm) was triggered with blue light pulses (488 nm, intensity 1%) every 5.3 s, in order to minimize undesired photobleaching effects. The mean fluorescence intensity of a whole GUV was quantified using ImageJ.

mOrange-Nano recruitment to disiLID/iLID functionalized SLBs

Each well of the µ-slide 18 well glass-bottom chambers was activated with 150 µL of 2 M NaOH for 1 h. Subsequently, the NaOH solution was removed and the wells were washed 3 times with 150 µL Milli-Q water and then with 150 µL buffer (50 mM Tris pH 7.4, 100 mM NaCl) solution containing 10 mM $CaCl_2$. Subsequently, 15 µL of SUVs (1mg/mL) solution was added to 150 µL of buffer and the chamber was incubated for 30 min at room temperature. The formed SLBs were washed 5 times with buffer by removing and adding 80 µL of buffer in each step.

For their functionalization, the SLBs were incubated with 250 nM SAv for 30 min and subsequently, the excess SAv was removed by washing with buffer 5 times. Afterwards,

1 μM of either b-iLID or b-disiILD was incubated with the SLB for 30 min, and the excess was removed by washing with buffer 5 times.
Under the fluorescence microscope, 200 nM mOrange-Nano were added on top of the functionalized SLBs. The quality of the SLBs was verified in the DiD channel. mOrange-Nano was recruited to selected ROIs with blue light pulses (488 nm, intensity 1%) every 2.6 s.

Fluorescence recovery after photobleaching (FRAP)

After preparing SLBs as described, the SLBs were incubated with 250 nM SAv-Cy3 for 30 min and subsequently, the excess SAv was removed by washing with buffer 5 times. The sample was placed in the confocal microscope and the FRAP Wizard interface in the LAS X software was selected for FRAP measurements. A region of interest (ROI) of 13.3 μm diameter was defined for pre-bleach, bleach, and postbleach sequences. Overall, 5 frames during pre-bleach, 5 frames during bleach, and 300 frames at post-bleach were acquired with 0.38 s intervals, followed by acquisition of additional 120 frames with 1 s intervals. Laser power was set at 100% for 552 nm and 638 nm lasers for bleach. Fluorescence intensities were measured in LAS X software to generate recovery curves and data were fit to the first order exponential. Half-lives ($t_{1/2}$) of fluorescence recovery was calculated by using $t_{1/2} = \ln(2)*\tau$ and apparent diffusion coefficient (D) was calculated by the formula $D = (0.88\omega^2)/4 \cdot t_{1/2}$, where ω is the radius of the bleached ROI.

Figures and graphs

Figure 1 in the main text was created with BioRender.com. Graphs were made with OriginPro 2020.

Supporting Figures

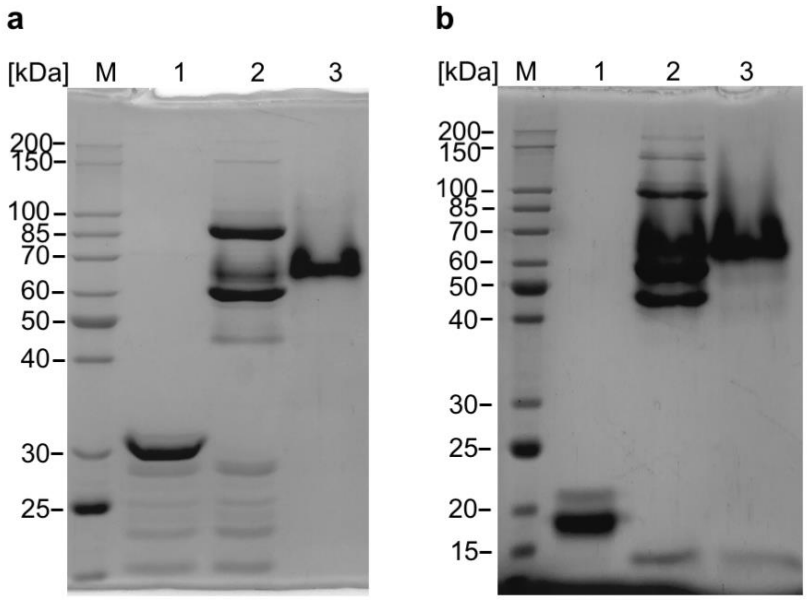

Figure S1. SDS-PAGE of purified a) b-disiLID and b) b-iLID. M: Marker (NEB, Catalogue No.: S771S), 1: purified protein, 2: purified protein (650 pmol) + SAv (4.72 nmol tetramer), 3: SAv. All proteins were visualized using a Coomassie stain. The addition of SAv to the biotinylated proteins results in the disappearance of the original band in 1 and the formation of a higher molecular weight band in 2, proving the complete biotinylation of the proteins b-iLID and b-disiLID.

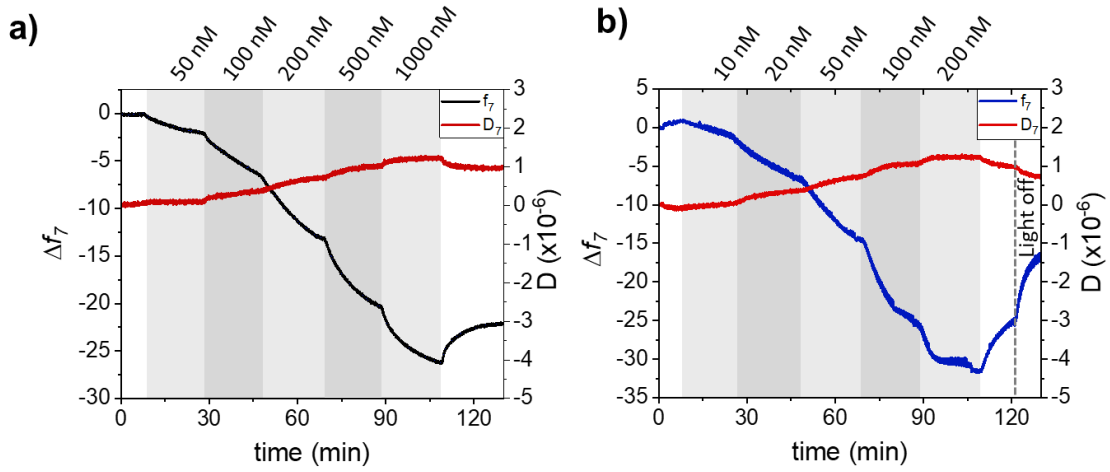

Figure S2. QCM-D curves for the titration of disiLID-functionalized SLB with increasing concentrations of Nano a) in the dark and b) under blue light. Gray areas indicate the binding steps, while white areas indicate buffer wash. All steps were performed under flow.

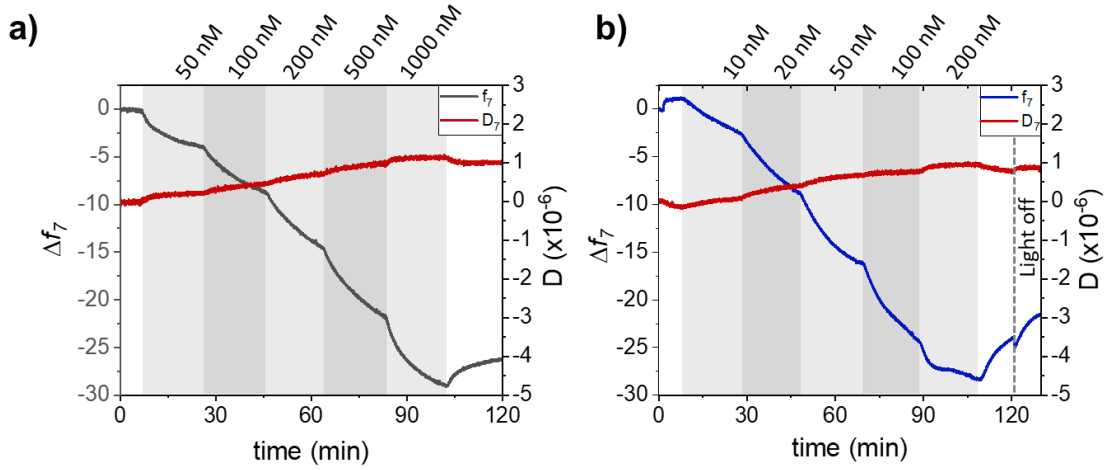

Figure S3. QCM-D curves for the titration of iLID-functionalized SLB with increasing concentrations of Nano a) in the dark and b) under blue light. Gray areas indicate the binding steps, while white areas indicate buffer wash. All steps were performed under flow.

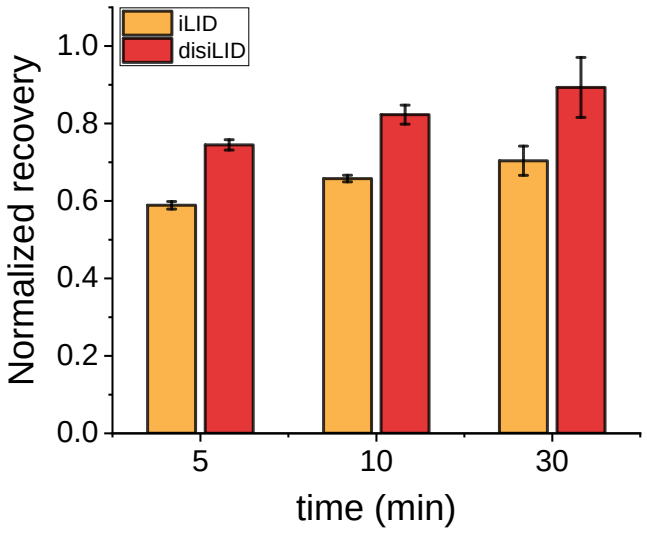

Figure S4. Normalized recovery in frequency after interruption of blue light illumination in QCM-D measurements, corresponding to the desorption of Nano from iLID- (orange) or disiLID- (red) functionalized SLBs. Values represent the average of 3 independent measurements ± STD.

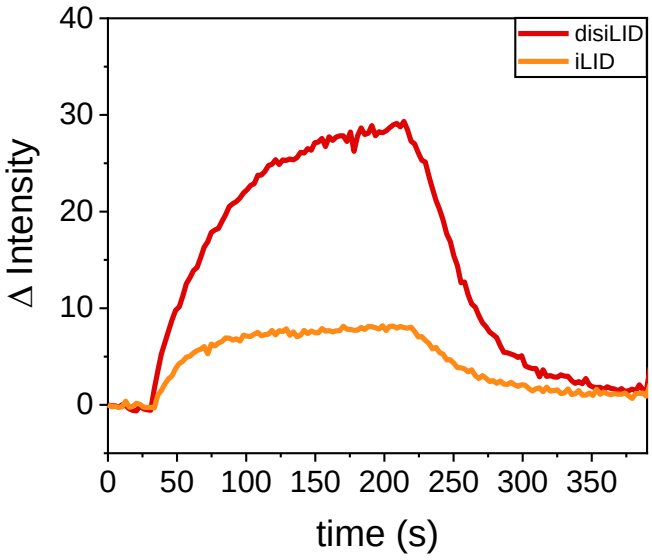

Figure S5. Fluorescence intensity of mOrange recruited on SLBs decorated with b-disiLID (red) or b-iLID (yellow) over time.

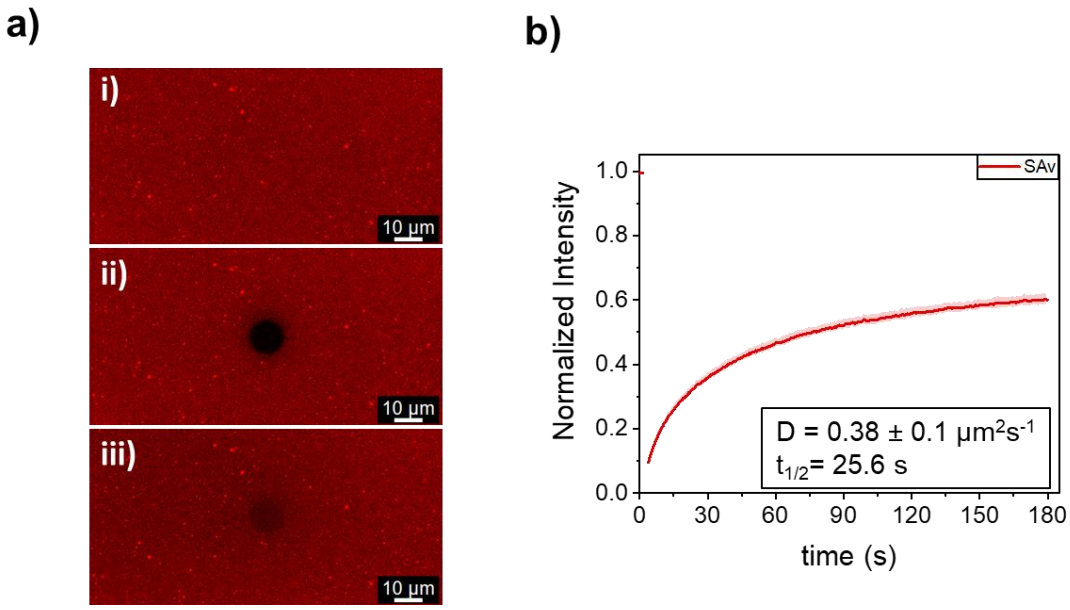

Figure S6: FRAP images in Cy3 channel of SLBs containing DOPC with 5 mol% DOPE-biotin and functionalized with SAv-Cy3. a) Fluorescence images of SAv-functionalized SLB before bleaching (i), after bleaching (ii) and after 180 s recovery (iii). b) Normalized fluorescence intensity after photobleaching in the Cy3 channel. (n=6, mean ± STD).

Supplementary Sequences

pQE-80L iLID-AviTag (AviTag, His6-tag, iLID)

>Amino acid sequence

MGGSGLNDIFEAQKIEWHEGGSHHHHHHGSGEFLATTLERIEKNFVITDPRLPD
NPIIFASDSFLQLTEYSREEILGRNCRFLQGPETDRATVRKIRDAIDNQTEVTVQLI
NYTKSGKKFWNVFHLQPMRDYKGDVQYFIGVQLDGTERLHGAAEREAVMLIK
KTAFQIAEAANDENYF

>Nucleic acid sequence

ATGGGTGGTTCCGGCCTGAACGATATCTTCGAAGCGCAGAAGATTGAATGGC
ACGAAGGTGGTTCCCATCACCATCACCATCACGGATCCGGGGAGTTTCTGGC
AACCACACTGGAACGGATCGAGAAAAATTTCGTGATTACTGATCCGAGACTG
CCTGACAACCCAATCATTTTTGCGAGCGATTCCTTCCTGCAGCTGACAGAATA
TTCTCGGGAAGAGATCCTGGGGCGCAATTGCCGTTTTCTGCAGGGACCCGAG
ACAGACCGTGCCACTGTTCGGAAAATCAGAGATGCTATTGACAACCAGACTG
AAGTGACCGTTCAGCTGATCAATTATACCAAGAGCGGCAAGAAGTTCTGGAA
CGTGTTCCACCTGCAGCCGATGCGCGATTATAAGGGCGACGTCCAGTACTTC
ATTGGCGTGCAGCTGGATGGCACCGAACGTCTTCATGGCGCCGCTGAGCGTG
AGGCGGTCATGCTGATCAAAAAGACAGCCTTTCAGATTGCTGAGGCAGCGA
ACGACGAAAATTACTTTTAA

pET21_dis-iLID-AviTag AviTag, His6-tag, disordered domain from OSBP, iLID

>Amino acid sequence

MGGSGLNDIFEAQKIEWHEGGSHHHHHHGSMAATELRGVVGPGPAAIAALGG
GGAGPPVGGGGGRGDAGPGSGAASGTVVAAAAGGPGPGAGGVAAAGPPAPPT
GGSGGSGAGGSGSAGEFLATTLERIEKNFVITDPRLPDNPIIFASDSFLQLTEYSRE
EILGRNCRFLQGPETDRATVRKIRDAIDNQTEVTVQLINYTKSGKKFWNVFHLQ
PMRDYKGDVQYFIGVQLDGTERLHGAAEREAVMLIKKTAFQIAEAANDENYF

>Nucleic acid sequence

ATGGGTGGTTCCGGCCTGAACGATATCTTCGAAGCGCAGAAGATTGAATGGC

ACGAAGGTGGTTCCCATCACCATCACCATCACGGTTCCATGGCAGCTACAGA
ACTAAGGGGAGTTGTAGGTCCGGGTCCGGCTGCGATCGCCGCGCTGGGTGGT
GGCGGTGCGGGCCCACCGGTTGGTGGCGGCGGTGGCCGTGGTGACGCAGGC
CCGGGTTCGGGTGCCGCTAGCGGCACCGTTGTGGCCGCGGCGGCGGGTGGC
CCTGGTCCGGGTGCGGGTGGGGTGGCAGCGGCGGGTCCGCCGGCACCGCCG
ACGGGTGGTAGCGGCGGCTCTGGCGCTGGCGGCTCCGGCAGCGCAGGGGAG
TTTCTGGCAACCACACTGGAACGGATCGAGAAAAATTTCGTGATTACTGATC
CGAGACTGCCTGACAACCCAATCATTTTTGCGAGCGATTCCTTCCTGCAGCT
GACAGAATATTCTCGGGAAGAGATCCTGGGGCGCAATTGCCGTTTTCTGCAG
GGACCCGAGACAGACCGTGCCACTGTTCGGAAAATCAGAGATGCTATTGAC
AACCAGACTGAAGTGACCGTTCAGCTGATCAATTATACCAAGAGCGGCAAGA
AGTTCTGGAACGTGTTCCACCTGCAGCCGATGCGCGATTATAAGGGCGACGT
CCAGTACTTCATTGGCGTGCAGCTGGATGGCACCGAACGTCTTCATGGCGCC
GCTGAGCGTGAGGCGGTCATGCTGATCAAAAAGACAGCCTTTCAGATTGCTG
AGGCAGCGAACGACGAAAATTACTTTTAA

Supporting References

[1] G. Guntas, R. A. Hallett, S. P. Zimmerman, T. Williams, H. Yumerefendi, J. E. Bear, B. Kuhlman, *Proceedings of the National Academy of Sciences* **2015**, *112*, 112-117.

[2] S. M. Bartelt, E. Chervyachkova, J. Steinkühler, J. Ricken, R. Wieneke, R. Tampé, R. Dimova, S. V. Wegner, *Chemical Communications* **2018**, *54*, 948-951.

[3] D. Di Iorio, Y. Lu, J. Meulman, J. Huskens, *Chemical Science* **2020**, *11*, 3307-3315.

[4] A. Weinberger, F.-C. Tsai, Gijsje H. Koenderink, Thais F. Schmidt, R. Itri, W. Meier, T. Schmatko, A. Schröder, C. Marques, *Biophysical Journal* **2013**, *105*, 154-164.